January 2015

Brain cholesterol synthesis and metabolism is progressively disturbed in the R6/1 mouse model of Huntington's disease: a targeted GC-MS/MS sterol analysis

Fabian Kreilaus
University of Wollongong, fabian@uow.edu.au

Adena S. Spiro
University of Wollongong, adena@uow.edu.au

Anthony J. Hannan
University of Melbourne

Brett Garner
University of Wollongong, brettg@uow.edu.au

Andrew M. Jenner
University of Wollongong, ajenner@uow.edu.au

Brain cholesterol synthesis and metabolism is progressively disturbed in the R6/1 mouse model of Huntington's disease: a targeted GC-MS/MS sterol analysis

Abstract

Background:Cholesterol has essential functions in neurological processes that require tight regulation of synthesis and metabolism. Perturbed cholesterol homeostasis has been demonstrated in Huntington's disease, however the exact role of these changes in disease pathogenesis is not fully understood. Objective:This study aimed to comprehensively examine changes in cholesterol biosynthetic precursors, metabolites and oxidation products in the striatum and cortex of the R6/1 transgenic mouse model of Huntington's disease. We also aimed to characterise the progression of the physical phenotype in these mice. Methods:GC-MS/MS was used to quantify a broad range of sterols in the striatum and cortex of R6/1 and wild type mice at 6, 12, 20, 24 and 28 weeks of age. Motor dysfunction was assessed over 28 weeks using the RotaRod and the hind-paw clasping tests. Results:24(S)-Hydroxycholesterol and 27-hydroxycholesterol were the major cholesterol metabolites that significantly changed in R6/1 mice. These changes were specifically localised to the striatum and were detected at the end stages of the disease. Cholesterol synthetic precursors (lathosterol and lanosterol) were significantly reduced in the cortex and striatum by 6 weeks of age, prior to the onset of motor dysfunction, as well as the cognitive and affective abnormalities previously reported. Elevated levels of desmosterol, a substrate of delta(24)-sterol reductase (DHCR24), were also detected in R6/1 mice at the end time-point. Female R6/1 mice exhibited a milder weight loss and hind paw clasping phenotype compared to male R6/1 mice, however, no difference in the brain sterol profile was detected between sexes. Conclusion:Several steps in cholesterol biosynthetic and metabolic pathways are differentially altered in the R6/1 mouse brain as the disease progresses and this is most severe in the striatum. This provides further insights into early molecular mediators of HD onset and disease progression and identifies candidate molecular targets for novel therapeutic approaches.

Publication Details

Kreilaus, F., Spiro, A. S., Hannan, A. J., Garner, B. & Jenner, A. M. (2015). Brain cholesterol synthesis and metabolism is progressively disturbed in the R6/1 mouse model of Huntington's disease: a targeted GC-MS/MS sterol analysis. Journal of Huntington's Disease, 4 (4), 305-318.

Brain cholesterol synthesis and metabolism is progressively disturbed in the R6/1 mouse model of Huntington's disease – A targeted GC-MS/MS sterol analysis

Fabian Kreilaus[a,b,*], Adena S. Spiro[a,b], Anthony J. Hannan[c,d], Brett Garner[a,b], and Andrew M. Jenner[a,b]

[a]Illawarra Health and Medical Research Institute, University of Wollongong, NSW 2522, Australia

[b]School of Biological Sciences, University of Wollongong, NSW 2522, Australia

[c]Florey Institute of Neuroscience and Mental Health, University of Melbourne, Parkvillie, VIC, Australia

[d]Department of Anatomy and Neuroscience, University of Melbourne, Parkville, VIC, Australia.

*Corresponding author: Tel.: +61-402195891, Email: fk628@uowmail.edu.au

Keywords: Huntington's disease; Cholesterol; Biological Markers; Tandem Mass Spectrometry; 24-hydroxycholesterol; cholesterol 24-hydroxylase

Running title: Brain cholesterol dysregulation in R6/1 mice

Abstract

Background: Cholesterol has essential functions in neurological processes that require tight regulation of synthesis and metabolism. Perturbed cholesterol homeostasis has been demonstrated in Huntington's disease, however the exact role of these changes in disease pathogenesis is not fully understood.

Objective: This study aimed to comprehensively examine changes in cholesterol biosynthetic precursors, metabolites and oxidation products in the striatum and cortex of the R6/1 transgenic mouse model of Huntington's disease. We also aimed to characterise the progression of the physical phenotype in these mice.

Methods: GC-MS/MS was used to quantify a broad range of sterols in the striatum and cortex of R6/1 and wild type mice at 6, 12, 20, 24 and 28 weeks of age. Motor dysfunction was assessed over 28 weeks using the RotaRod and the hind-paw clasping tests.

Results: 24-Hydroxycholesterol and 27-hydroxycholesterol were the major cholesterol metabolites that significantly changed in R6/1 mice. These changes were specifically localised to the striatum and were detected at the end stages of the disease. Cholesterol synthetic precursors (lathosterol and lanosterol) were significantly reduced in the cortex and striatum by 6 weeks of age, prior to the onset of motor dysfunction, as well as the cognitive and affective abnormalities previously reported. Elevated levels of desmosterol, a substrate of delta(24)-sterol reductase (DHCR24), were also detected in R6/1 mice at the end time point. Female R6/1 mice exhibited a milder weight loss and hind paw clasping phenotype compared to male R6/1 mice, however, no difference in the brain sterol profile was detected between sexes.

Conclusion: Several steps in cholesterol biosynthetic and metabolic pathways are differentially altered in the R6/1 mouse brain as the disease progresses and this is most severe

in the striatum. This provides further insights into early molecular mediators of HD onset and disease progression and identifies candidate molecular targets for novel therapeutic approaches.

Introduction

Huntington's disease (HD) is a progressive neurodegenerative disease caused by the expansion of a trinucleotide [cytosine-adenine-guanidine (CAG)] repeat on the N-terminus of the huntingtin protein (HTT). The classical neuropathological hallmark of HD is the severe atrophy of the striatum (caudate and putamen) [1], with substantial volume loss in the order of 50%. This primarily manifests as involuntary movements (chorea) and cognitive dysfunction. MRI techniques have also highlighted that the hippocampus, cerebral cortex, globus pallidus and amygdala also have reduced volume in HD patients [2]. Among other effects, the expansion of the CAG repeat on *HTT* has been reported to alter HTT-phospholipid interactions [3], membrane organisation [4] and gene transcription of lipid metabolic enzymes [5]. Several studies have also identified that cholesterol synthesis and metabolism in HD cell lines and animal models is significantly disturbed [6-8] highlighting possible mechanisms. However, further investigation into different sterol-related mechanisms and metabolic pathways is necessary to examine their influence on HD pathophysiology.

Cholesterol is highly concentrated in the brain, the majority found in myelin, accounting for 70% of total cholesterol, with the remainder found in cellular membranes of neurons and glial cells. Maintenance of cholesterol levels is essential for many neurological functions including dendritic maintenance [9], synaptogenesis [10] and axon growth [11]. Genetic defects that alter cholesterol synthetic enzymes can have severe consequences [12,13], especially in the brain where tight regulation of cholesterol synthesis is essential for normal neuronal function.

The blood brain barrier (BBB) is impermeable to cholesterol, preventing fluctuations in circulating cholesterol affecting brain levels. Brain cholesterol is derived from *de novo* synthesis, a pathway that involves over 20 steps. Cholesterol biosynthetic regulation is thought to involve a complex interplay between sterol sensing elements [sterol regulatory element-binding proteins (SREBPs)] and transcription factors responsible for producing cholesterol synthetic enzymes [14]. However, recent evidence suggests that further regulation of cholesterol synthesis may occur in the later stages of the pathway [15,16]. The later stages of the cholesterol biosynthetic pathway are branched into the Kandutsch-Russell and Bloch pathways. Several cholesterol synthetic precursors exist in these pathways that occur downstream of squalene (see Fig. 1). Although the rate of cholesterol synthesis in peripheral tissues can be estimated by plasma levels of cholesterol synthetic precursors (lathosterol and lanosterol), these do not reflect central nervous system (CNS) cholesterol synthesis. Direct measurement of sterol precursor levels in brain tissue is therefore necessary to monitor the cholesterol synthetic pathway [7,8,17].

24-Hydroxycholesterol (24-OHC) has been marked as a molecule of interest after being identified as a major and specific elimination product of cholesterol from the brain [18,19]. Side chain hydroxylation of cholesterol increases membrane permeability and enables movement across the BBB into circulation. 24-OHC is formed enzymatically from CNS cholesterol catalysed by cholesterol 24-hydroxylase (CYP46A1), which is primarily expressed in neurons [20]. Plasma 24-OHC levels have been suggested as a marker of metabolically active neurons in the brain [19], and have been shown to be reduced in the plasma of HD patients [21,22] and in brain tissue of several rodent models of HD [8]. Furthermore, an association between altered CYP46A1 activity and 24-OHC levels has been reported in other neurodegenerative diseases [23-26], however the role of these changes in HD pathogenesis are unknown.

27-Hydroxycholesterol (27-OHC) is a major metabolic product of cholesterol in peripheral tissue, entering the bloodstream to be further metabolised in the liver [27,28]. The enzyme cholesterol 27-hydroxylase (CYP27A1) catalyses the formation of 27-OHC. A concentration gradient results in a net movement of 27-OHC from circulation into the brain [29], where it is quickly metabolised into more polar products (including dihydroxysterols and cholestenoic acids), catalysed by CYP27A1 and 5-hydroxycholesterol 7-α-hydroxylase (CYP7B1) [30]. Although 27-OHC has been reported to be elevated in Alzheimer's disease (AD) brain tissue [31,32], the importance of this metabolic pathway has not been established in other neurodegenerative diseases, including HD.

Oxidative damage to biological macro molecules is a major component of neurodegenerative diseases, including AD [33] and Parkinson's disease (PD) [34]. Free radical mediated oxidation of cholesterol in the 5,6 position forms 7β-hydroxycholesterol (7β-OHC) and 7-ketocholesterol (7-KC). An elevation of these cholesterol oxidation products (COPs) has been reported in several diseases and pathological models that involve oxidative stress [35-38]. Due to the high concentration of cholesterol in the brain, COPs represent potentially important biomarkers for oxidative stress in neurodegenerative diseases.

Perturbed cholesterol synthetic and metabolic pathways have been previously reported in HD mouse and cell models [5-7,17]. Due to the complexity of the cholesterol synthetic pathway, previous studies have measured some of the major brain synthetic sterol intermediates and metabolites, but the full extent of potential sterol alterations that may occur in different brain regions has not been fully examined. In this study we have used an accurate and sensitive GC-MS/MS technique to characterise cholesterol pathway alterations occurring in the striatum and cortex of the R6/1 mouse model. Physical phenotypic changes were also examined including, impaired motor performance, weight loss, reduced brain mass and involuntary clasping. Analysis of multiple time points and two different brain regions aimed

to establish when specific alterations of cholesterol synthetic and metabolic pathways may occur during the progression of HD in the R6/1 mouse model.

Materials and Methods

Materials

Desmosterol-d_6, zymosterol-d_5, zymosterol and lanosterol-d_6 were obtained from Avanti lipids (Alabaster, AL, USA). Tert-butylhydroxytoluene (BHT), cholesterol, α-cholestane, 7β-hydroxycholesterol, 7-dehydrocholesterol and 7-ketocholesterol were from Sigma (St. Louis, MO, USA). Lathosterol, lanosterol, desmosterol and 27-hydroxycholesterol were obtained from Steraloids (Newport, RI, USA). 7β-hydroxycholesterol-d_7, lathosterol-d_4 and 7-ketocholesterol-d_7 were purchased from CDN Isotopes (Quebec, Canada). 27-hydroxycholesterol-d_5, 24-hydroxycholesterol and 24-hydroxycholestero-d_7 were from Medical Isotopes, Inc (Pelham, AL, USA). 24,25-dihydrolanosterol-d_6 was obtained from Toronto research chemicals (TRC, Ontario, Canada). All standards obtained were of the highest purity (>95%). Methanol, hexane, methyl tert-butyl ether (MTBE), acetonitrile, toluene, formic acid and NaOH were purchased from Ajax Finechem (Thermo Fisher Scientific, AU). CUQAX223 UCT Clean-Up QAX2 solid phase extraction columns and BSTFA (N,O-bis(trimethylsilyl) trifluoroacetamide) + 1% TMCS (trimethylchlorosilane) was purchased from PM Separations (Qld, Australia).

Mice

Transgenic R6/1 male mice were provided by the Hannan Laboratory, Florey Institute of Neurosciences and Mental Health, and bred with CBB6 (CBA x C57/B6) F_1 female mice at Australian Bio-Resources (Mossvale, Australia). Equal numbers of male and female R6/1 and

wild type mice were housed in standard small rodent cages. At least two of each genotype was housed per cage. Mice were provided with standard rodent diet ("rat & mouse nut", Vella Stock Feeds, NSW, Australia) and water available *ad libitum*. Body weight was recorded every 4-5 days from 7 weeks until sacrifice. All procedures that were undertaken conformed to the standards of the University of Wollongong ethics committee (animal ethics approval number: AE 13/20).

Behavioural testing

A RotaRod apparatus (TSE systems, Bad Homberg, Germany) was used to measure motor performance of mice. Mice were acclimatised to the RotaRod over two days before initial testing. The testing protocol involved a rotation of 4 RPM for 5 sec followed by a linear acceleration from 4 to 40 RPM over 200 sec. The latency to fall was measured automatically by the RotaRod using light beam sensors. This procedure was repeated (5 times in total) and the average of the two longest run times was recorded for analysis. The hind paw clasping phenotype was tested by suspending the mouse by the tail. Mice that clasped both hind paws tightly to their body were considered to have a complete clasp phenotype. Mice that clasped one paw or both paws in an interrupted manner were considered to have a "half clasp" phenotype.

Brain tissue collection

Mice were euthanised using slow flow CO_2 asphyxiation and perfused with 1 x PBS (4^{o}C). The head was then excised and the whole brain removed and weighted. Cerebral cortex and striatum was dissected and snap frozen in liquid N_2 and stored at -80^{o}C prior to analysis.

Lipid extraction

Frozen brain tissue (~5-10 mg) was weighed directly into a 0.5 mL polypropylene tube containing 5 Zircosil® ceramic beads (1.3 mm) (Klausen Pty Ltd, NSW, Australia), 150 µL

methanol (0.01% BHT) and internal standards (4°C). Tissue was homogenised at 4°C using a Precellys 24 homogeniser (Bertin Technologies) (2 x 20 s at 5,000 rpm) and the homogenate was transferred to a clean glass vial. The tube and ceramic beads were washed with 100 µL methanol (4°C) and was added to the homogenate with 250 µL of NaOH (1 M). The sample was hydrolysed at room temperature for 16 h in the absence of light and then acidified with 330 µL of 1 M formic acid. The sample was made up to a final volume of 3 mL (8% methanol, pH 4.5) by the addition of 2.2 mL milliQ water. Solid-phase extraction (SPE) was carried out on a 200 mg mixed C8/anion exchange quaternary amine column (CUQAX223, UCT Inc.) that had been preconditioned with 2 mL methanol and then 2 mL 40 mM formic acid buffer (pH 4.5). The lipid extract was loaded and the column washed with 2 mL methanol in 40 mM formic acid (40:60). The SPE column was dried with N_2 gas flow for 5 min. Sterols and oxysterols were eluted in a single fraction with 2 mL hexane followed by 2 mL hexane/MTBE (50:50).

GC-MS/MS sterol analysis

The sterol/oxysterol fraction was dried under N_2 gas flow at 37°C and derivatised by the addition of 20 µL acetonitrile and 20 µL BSTFA + 1% TMCS for one hour at 37°C. Samples were dried under N_2 and immediately reconstituted in 40 µL toluene for GC-MS/MS analysis. Selective reaction monitoring (SRM) analysis of sterols/oxysterols was carried out on an Agilent 7000B triple quadrupole mass selective detector interfaced with an Agilent 7890A GC system gas chromatograph. Quantification was performed by Agilent Masshunter Quantitative software (V B.05.00) by comparison of specific SRM transitions with their corresponding heavy isotopes and using relative response factor calibration. Cholesterol was quantified using the internal standard α-cholestane in a separate injection and chromatographic run.

Statistical analysis

Linear regression analysis was used to identify the rate of weight gain between genotypes and identify the relationship between age and sterol changes in mice. A 2-way ANOVA was used to analyse RotaRod performance, body weight, brain lipid and brain mass data, with Bonferroni post-tests to compare means at individual time points. A student's t test was also used to compare sterols levels between sexes and at individual time points in the sterol data. *P*-values < 0.05 were considered significant. All analyses were performed in Graphpad PRISM v5.0 (Graphpad Software Inc., USA).

Results

Physical phenotype

The cohort of R6/1 and WT littermates housed until 28 weeks of age (n = 5 per genotype and sex) were tested periodically for physical changes that characterise the progression of the HD phenotype. These results are represented in Fig. 2.

Weight loss in R6/1 mouse

Male and female R6/1 body weight was significantly reduced compared to WT mice over the course of the study ($p < 0.0001$, Fig. 2A). The mean body weight of R6/1 mice did not increase after 16 weeks of age in males, and 19 weeks in females. Prior to weight loss (7-19 weeks) the rate of weight gain was significantly less in female R6/1 mice compared to WT ($p = 0.00012$). No significant difference in the rate of weight gain was detected between male R6/1 and WT mice in the 6-16 week period. By 28 weeks the average weight increase from the earliest measurement (7 weeks) was 8% in R6/1 males and 19% in R6/1 females.

Hind-paw clasping phenotype

The hind-paw clasping phenotype was previously observed in R6/1 and R6/2 mice [39]. In our study the clasping phenotype was first observed at 12 weeks in males (Fig. 2B), with the percentage of mice showing positive for the phenotype increasing to 60% at the end of the study. Female R6/1 mice first exhibited the clasping phenotype at the age of 17 weeks (Fig. 2B). The percentage of female R6/1 mice showing the phenotype increased to 60% by the end of the study. A small proportion of WT mice showed a positive "half clasp" phenotype at varying times throughout the study.

Motor performance

The average latency to fall from the RotaRod was significantly less in R6/1 mice compared to WT in both males ($p = 0.0016$) and females ($p = 0.0004$) over the course of the study (Fig. 2C). No difference in the RotaRod performance was detected between genders of the same genotype.

Brain mass

The brain mass of both male and female R6/1 mice was significantly less than WT littermates at later time points (Fig. 3). The difference between WT and R6/1 male mice was highly significant at 20, 24 and 28 weeks ($p < 0.0001$). In female mice a significant difference was detected at 12 and 20 weeks ($p < 0.05$), becoming highly significant at 24 and 28 weeks ($p < 0.0001$).

Sterol analysis of R6/1 brain tissue

Tissues from both male and female R6/1 and WT mice were investigated in the sterol analysis. Minor differences in the sterol profile between male and female mice of the same genotype were identified (Supplemental Table 1-2), however these did not influence the

differences identified between WT and R6/1 mice. Therefore to increase statistical power, both sexes were combined and reanalysed. The level of all sterols measured for the individual sexes can be found in Supplemental Table 1-2. The following results summarise the data for combined sexes.

Cholesterol synthetic precursors

Several cholesterol synthetic precursors were significantly decreased in R6/1 striatum and cortex compared to WT (Figs. 3.5A-D, 3.6A-D). Lathosterol levels were significantly reduced from the pre-symptomatic age of 6 weeks in R6/1 striatum ($p < 0.001$) and cortex ($p < 0.05$) when compared to WT mice. Lathosterol was consistently reduced in both cortex and striatum of R6/1 mice compared to WT at all later time points (12, 20, 24 and 28 weeks; $p < 0.001$, Figs. 4A, 5A). Lanosterol and zymosterol followed a similar consistent reduction; a significant difference in lanosterol levels was first detected at 12 weeks in striatum (Fig. 4B) and cortex (Fig. 5B) of R6/1 (striatum $p < 0.01$, cortex $p < 0.05$). R6/1 striatum exhibited an early reduction in zymosterol at 6 weeks ($p < 0.01$), and at all later time points (Fig. 4C). The level of zymosterol in cortex tissue was only significantly reduced compared to WT at 28 weeks of age ($p < 0.05$, Fig. 5C). The cholesterol synthetic precursor 24,25 dihydro lanosterol was not significantly altered in the R6/1 striatum or cortex although it was detected at lower mean levels than WT at all time-points examined (Figs. 4D, 5D).

Lathosterol, lanosterol, zymosterol and 24,25 dihydro lanosterol levels decreased over time in the striatum of both WT and R6/1 mice (Fig. 4A-D, $p < 0.01$). In the cortex, lanosterol, zymosterol and 24, 25 dihydro lanosterol decreased significantly over time in R6/1 mice but not WT (Fig. 5B, C, D, $p < 0.05$). Lathosterol decreased significantly over time in the cortex of both R6/1 and WT mice (Fig. 5A, $p < 0.05$).

Unlike upstream sterols in the cholesterol synthetic pathway, desmosterol levels did not significantly decrease over time in the striatum of R6/1 mice (Fig. 4E). Comparing the means between R6/1 and WT mice at individual time points identified desmosterol was significantly elevated in R6/1 striatum at 20 and 28 weeks compared to WT (t-test, $p = 0.046$ and $p = 0.0138$ respectively, Fig. 4E). Desmosterol levels in cortex were also unaltered over time in both WT and R6/1 mice. A small but significant elevation of desmosterol was detected in R6/1 mice at 28 weeks (t-test, $p = 0.0431$, Fig. 5E). 7-dehydrocholesterol levels did not decrease over time in cortex or striatum of R6/1 mice, and no difference between R6/1 and WT mice was detected at any time point (Figs. 4F, 5F).

Cholesterol

Total cholesterol levels were not significantly altered between R6/1 and WT mice in this study. However, an increase in cholesterol levels over time (6-28 weeks of age) was observed both in striatum and cortex of WT and R6/1 mice ($p < 0.05$, Fig. 6).

Cholesterol metabolites

The brain specific cholesterol elimination product 24-OHC was significantly reduced in the striatum of R6/1 mice at the end time point of 28 weeks ($p < 0.01$, Fig. 6). No other time point or brain region measured showed an effect of genotype on 24-OHC levels. 24-OHC levels increased in both striatum and cortex of WT and R6/1 mice over time ($p < 0.01$, Fig. 6).

27-OHC, a predominantly peripheral metabolite of cholesterol was consistently reduced in R6/1 striatum from the age of 12 weeks ($p < 0.05$) and at all later time points (20 weeks $p < 0.01$, 24 weeks $p < 0.05$, 28 weeks $p < 0.05$, Fig. 6). 27-OHC levels were not significantly altered in cortex tissue of R6/1 mice when compared to WT at any of the 5 time-points examined (Fig. 6).

Cholesterol oxidation products

Free radical generated oxidation products of cholesterol were also measured over the course of the study. No significant differences in the level of 7-KC and 7β-OHC were detected between R6/1 and WT in any brain region or timepoint measured (Supplemental Table 1-3).

Discussion

This is the first study to comprehensively examine progressive sterol changes in the R6/1 mouse model, and has investigated a greater number of cholesterol synthetic precursors and metabolites than other studies of HD animal models to date. Previous studies examining cholesterol changes in HD mouse models have focused on several major sterols in whole brain homogenates at multiple time-points during disease progression, or in specific brain regions at a single time-point. Recent studies suggesting more complex cholesterol synthetic regulation in the later stages of the cholesterol synthetic pathway [15,16] highlights the relevance of this study investigating a wider variety of cholesterol synthetic precursors.

Minor sterol differences between sexes did not influence differences detected between R6/1 and WT mice. Therefore, for simplicity the following discussion describes changes occurring when sexes were combined. The significant reduction of lathosterol and zymosterol in the striatum of R6/1 mice at 6 weeks of age represents the earliest detectable change in the R6/1 sterol profile, and appears before the onset of overt motor dysfunction as measured on the RotaRod. In fact, 6 weeks of age in R6/1 mice also precedes the onset of cognitive deficits [40,41] and affective abnormalities [42,43] in this HD model and therefore this sterol dysregulation could contribute to cognitive, psychiatric and motor symptoms. Changes to zymosterol are more specific to the striatum compared to other precursors that decrease early

in both cortex and striatum. This highlights zymosterol as a possible specific biomarker of early striatal changes in HD mice.

Synthetic precursor levels were more severely affected in striatum compared to cortex in our study; changes occurred earlier and were of a greater magnitude in striatum (lathosterol decreased by 80% in striatum compared with 50% in cortex). This observation is consistent with previous studies in the yeast artificial chromosome (YAC 128) and R6/2 transgenic HD mouse models [7,17]. The striatum is also the earliest and most severely affected region in HD [1]. Absolute cholesterol and cholesterol synthetic precursor levels have been shown to be higher in striatum compared to cortex [7,44], and for this reason it has been hypothesised that disturbed cholesterol homeostasis in HD may lead to specific vulnerability of the striatum [7]. Significant sterol changes early in the striatum of the R6/1 mouse suggest that alterations to the cholesterol biosynthetic pathway in the brain occur very early; with the possibility that these changes may even be present during embryonic development. Since the majority of brain cholesterol is synthesised during prenatal life [45], HD neurodegeneration may be seeded early, with individuals only becoming symptomatic later in life. A current hypothesis suggests that errors in myelination during development may be a factor in human HD, taking many years to manifest before onset due to compensatory mechanisms that function early but become overwhelmed in the aged brain [46]. Alternatively, early changes to cholesterol biosynthesis may be independent of the pathological processes in this HD model.

This study has also examined 7-dehydrocholesterol and desmosterol; the immediate precursors to cholesterol in the Kandutsch-Russell and Bloch pathways respectively (Fig. 1). Contrary to a previous finding that desmosterol decreases in symptomatic YAC 128 mice (10 months of age) [17], desmosterol levels were significantly elevated in R6/1 striatum and cortex by the end stage in our study. This may be a result of the different mouse models

expressing different forms of mutant HTT (truncated or full length). In addition, analytical discrimination of very similar sterols such as 7-dehydrocholesterol and desmosterol can be challenging. The use of GC-MS/MS in our study provides greater specificity than single quadrupole GC-MS that was used in the previous study [17]. Desmosterol elevation in R6/1 mice is unlikely a result of increased synthesis as cholesterol levels did not increase in our study or in a previous study examining R6/1 mice [4]. A plausible explanation for this accumulation is a reduced activity of the enzyme (DHCR24) that catalyses the conversion of desmosterol to cholesterol. Previous studies in R6/2 mice do not report desmosterol levels and therefore it is unknown if desmosterol accumulation also occurs in this related HD mouse model that expresses a longer CAG repeat in the R6 transgene [7]. 7-Dehydrocholesterol levels have not been previously reported in HD mouse brain, and in contrast to upstream Kandutsch-Russell branch precursors the levels were not significantly altered over time and between WT and R6/1 mice. Since lathosterol (the immediate precursor of 7-dehydrocholesterol) levels are substantially reduced the enzyme that converts 7-dehydrocholesterol to cholesterol (DHCR7) may also be less active or at lower abundance in R6/1 mice.

The absolute level of cholesterol synthetic precursors (lathosterol and lanosterol) in brain tissue has been proposed as a marker of the cholesterol synthetic rate [7,47]. However our results suggest there is likely to be more complex regulation at various points of the synthetic pathway (Fig. 1) than previously considered. Measurement of individual precursors alone to interpret synthetic rate may be potentially confounding. The cellular regulation of cholesterol synthesis occurring downstream of squalene has been investigated recently and identified the two terminal enzymes in the pathway interact functionally, DHCR24 regulating the activity of 7-dehydrocholesterol reductase (DHCR7) [16]. DHCR24 is also believed to have further regulatory roles upstream in the pathway [16], however these roles have not been fully

established and cholesterol synthetic regulation in the brain is still to be completely understood.

Consistent with previous studies in the striatum of R6/1 [4] and R6/2 mice [7], our study did not detect any significant alteration to the level of cholesterol in striatum and cortex of R6/1 mice compared to WT at any time-point. Previous studies also report conflicting results; a small but significant decrease in cholesterol levels was detected in whole brain of the YAC 128 mouse model [17], and a significant increase of total striatal cholesterol was detected in a knock-in mouse model [4]. These contradictions are probably due to differences in cholesterol quantification methodologies used, that have been shown to significantly affect the result obtained [48]. Analysis of different brain regions (striatum or whole brain homogenates) are also likely to produce different results as there can be up to a 3-fold difference in cholesterol levels between brain regions [7,44].

As WT and R6/1 mice aged, cholesterol synthetic precursor levels (lathosterol, lanosterol, zymosterol and 24,25 dihydro lanosterol) decreased in the striatum, and to a lesser extent the cortex. A similar reduction with age has been observed in human brain tissue [47]. An increase in cholesterol levels during aging suggests that metabolic pathways may also have a significant involvement in maintaining brain cholesterol levels, which has major implications for brain ageing, an overarching risk factor across all neurodegenerative brain diseases.

At 28 weeks of age a significant (25%) reduction of 24-OHC levels in the R6/1 striatum indicated that the relative decline of 24-OHC in R6/1 mice compared to WT is progressive over the course of the disease, becoming more pronounced at later stages. Previous studies have also identified a reduction of this metabolite in the brain and plasma of several other HD mouse models [7,8]. Here we have also identified that 24-OHC levels increase in cortex and striatum of R6/1 and WT during ageing, consistent with CYP46A1 enzyme levels increasing

with age in the mouse brain [20]. The importance of increased cholesterol metabolism in the ageing brain, and the potential effects of metabolic dysfunction in this HD model requires further investigation.

A predominantly peripheral metabolite of cholesterol, 27-OHC was also significantly reduced in R6/1 striatum by the age of 12 weeks, while cortex tissue had no significant alterations. 27-OHC has a net movement from circulation into the brain [29] and reduced levels seen in R6/1 mice might be explained by a whole body metabolic dysfunction that is known to occur in HD [49,50]. However, cortex tissue did not exhibit the same reduction of 27-OHC levels observed in striatum, and therefore it is possible that enzymes that further metabolise 27-OHC are upregulated, or enzymes capable of forming 27-OHC in brain are downregulated in striatum.

Oxidation of cholesterol in the 5,6 position generates 7β-OHC and 7-KC that have been demonstrated to be stable and reliable markers of oxidative stress, previously used in plasma [36]. In contrast to our results that showed no change in COPs, a study in the striatum of R6/1 mice did observe a time-dependant increase of lipid peroxidation using a less sensitive and specific lipid fluorescence based assay [51]. Since cholesterol is highly abundant in the brain, the presence of oxidative stress would be expected to increase the formation of COPs in the R6/1 mouse brain. Further research using oxidative damage biomarkers of multiple biomolecules in a variety of brain regions is required to understand the exact role that oxidative stress plays in the progression of HD pathophysiology.

Previous literature has typically studied either male or female R6/1 mice, in separate studies. Here we have examined both sexes in parallel between 6 and 28 weeks of age to more directly assess gender differences in the HD phenotype that have been previously reported.

Despite differences in human and mouse metabolism the CAG expansion in transgenic R6/1 mice causes weight loss in line with that observed in human HD patients [52,53]. Consistent with previous reports we observed a milder weight loss phenotype in females compared to male R6/1 mice [54,55]. Female R6/1 weight gain was significantly slower than WT mice prior to significant weight loss from 19 week of age, suggesting a metabolic abnormality from early life. Body weight of male R6/1 mice was variable and a significant difference in weight gain prior to weight loss was not detected. The primary cause of weight loss is unlikely due to lack of feeding since it has been reported that R6/1 mice have a similar food intake to WT mice whilst still exhibiting a distinct weight loss profile [39]. Food intake of R6/1 mice was not measured in this study to reduce stress on animals being isolated and reunited. During the progression of disease in R6/1 mice, both male and female mice showed a progressive loss of motor skills that were quantified by Rotarod. Despite the same environmental and handling conditions, high variation between mice reduced the statistical power and gender differences in the progression of the motor deficit could not be conclusively demonstrated. Impaired motor performance at the end time-point was comparable between male and female R6/1 mice.

In this study we have comprehensively profiled cholesterol synthetic and metabolic changes in R6/1 mice using GC-MS/MS and found similar reductions in the cholesterol synthetic precursors previously reported in the R6/2 model. The novel measurement of desmosterol and 7-dehydrocholesterol in R6/1 mice in this study has revealed potentially more complex dysregulation of the cholesterol synthetic pathway in HD. It has highlighted the specific accumulation of desmosterol in R6/1 brain tissue that is potentially due to reduced activity of DHCR24. Reduction of 24-OHC and 27-OHC in the striatum of R6/1 mice compared to WT littermates suggests that multiple pathways of cholesterol metabolism are perturbed in the R6/1 brain. Comprehensive and sensitive analysis of sterol compounds in the brain of R6/1

mice during progression of HD provides a new insight into synthetic and metabolic changes occurring in this model of HD. Novel data on age-related changes occurring in the brain also offers further information on sterol-related mechanisms that may influence other neurodegenerative processes that typically manifest in the aged brain.

Acknowledgements: The study was funded by a University of Wollongong start up grant (#1030328). F Kreilaus acknowledges his scholarship funding by The University of Wollongong and The Illawarra Health and Medical Research Institute. The authors also acknowledge the University of Wollongong statistical consulting service for providing advice on statistical analysis.

Author contributions: Conceived and designed experiments: A Jenner, F Kreilaus. Performed experiments: F Kreilaus, A Spiro. Analysed the data: F Kreilaus. Contributed reagents/materials/analysis tools: B Garner, A Jenner, A Hannan. Wrote the manuscript: F Kreilaus, A Spiro, A Jenner, A Hannan, B Garner.

Conflict of interest

The authors declare that they have no conflict of interest.

References

[1] Vonsattel JP, Myers RH, Stevens TJ, Ferrante RJ, Bird ED, Richardson EP, Jr. Neuropathological classification of Huntington's disease. J Neuropathol Exp Neurol. 1985 Nov;44(6):559-77.

[2] Rosas HD, Koroshetz WJ, Chen YI, Skeuse C, Vangel M, Cudkowicz ME, Caplan K, Marek K, Seidman LJ, Makris N, Jenkins BG, Goldstein JM. Evidence for more widespread cerebral pathology in early HD: an MRI-based morphometric analysis. Neurology. 2003 May 27;60(10):1615-20.

[3] Kegel KB, Sapp E, Alexander J, Valencia A, Reeves P, Li X, Masso N, Sobin L, Aronin N, DiFiglia M. Polyglutamine expansion in huntingtin alters its interaction with phospholipids. J Neurochem. 2009 Sep;110(5):1585-97.

[4] del Toro D, Xifro X, Pol A, Humbert S, Saudou F, Canals JM, Alberch J. Altered cholesterol homeostasis contributes to enhanced excitotoxicity in Huntington's disease. J Neurochem. 2010 Oct;115(1):153-67.

[5] Sipione S, Rigamonti D, Valenza M, Zuccato C, Conti L, Pritchard J, Kooperberg C, Olson JM, Cattaneo E. Early transcriptional profiles in huntingtin-inducible striatal cells by microarray analyses. Hum Mol Genet. 2002 Aug 15;11(17):1953-65.

[6] Valenza M, Rigamonti D, Goffredo D, Zuccato C, Fenu S, Jamot L, Strand A, Tarditi A, Woodman B, Racchi M, Mariotti C, Di Donato S, Corsini A, Bates G, Pruss R, Olson JM, Sipione S, Tartari M, Cattaneo E. Dysfunction of the cholesterol biosynthetic pathway in Huntington's disease. J Neurosci. 2005 Oct 26;25(43):9932-9.

[7] Valenza M, Leoni V, Tarditi A, Mariotti C, Bjorkhem I, Di Donato S, Cattaneo E. Progressive dysfunction of the cholesterol biosynthesis pathway in the R6/2 mouse model of Huntington's disease. Neurobiol Dis. 2007 Oct;28(1):133-42.

[8] Valenza M, Leoni V, Karasinska JM, Petricca L, Fan J, Carroll J, Pouladi MA, Fossale E, Nguyen HP, Riess O, MacDonald M, Wellington C, DiDonato S, Hayden M, Cattaneo E. Cholesterol defect is marked across multiple rodent models of Huntington's disease and is manifest in astrocytes. J Neurosci. 2010 Aug 11;30(32):10844-50.

[9] Fan QW, Yu W, Gong JS, Zou K, Sawamura N, Senda T, Yanagisawa K, Michikawa M. Cholesterol-dependent modulation of dendrite outgrowth and microtubule stability in cultured neurons. J Neurochem. 2002 Jan;80(1):178-90.

[10] Mauch DH, Nagler K, Schumacher S, Goritz C, Muller EC, Otto A, Pfrieger FW. CNS synaptogenesis promoted by glia-derived cholesterol. Science. 2001 Nov 9;294(5545):1354-7.

[11] Hayashi H, Campenot RB, Vance DE, Vance JE. Glial lipoproteins stimulate axon growth of central nervous system neurons in compartmented cultures. J Biol Chem. 2004 Apr 2;279(14):14009-15.

[12] Wassif CA, Maslen C, Kachilele-Linjewile S, Lin D, Linck LM, Connor WE, Steiner RD, Porter FD. Mutations in the human sterol Δ7-reductase gene at 11q12-13 cause Smith-Lemli-Opitz syndrome. Am J Hum Genet. 1998;63(1):55-62.

[13] Waterham HR, Koster J, Romeijn GJ, Hennekam RC, Vreken P, Andersson HC, FitzPatrick DR, Kelley RI, Wanders RJ. Mutations in the 3beta-hydroxysterol Delta24-reductase gene cause desmosterolosis, an autosomal recessive disorder of cholesterol biosynthesis. Am J Hum Genet. 2001 Oct;69(4):685-94.

[14] Brown MS, Goldstein JL. A proteolytic pathway that controls the cholesterol content of membranes, cells, and blood. Proc Natl Acad Sci U S A. 1999;96:11041-11048.

[15] Sharpe LJ, Brown AJ. Controlling cholesterol synthesis beyond 3-hydroxy-3-methylglutaryl-CoA reductase (HMGCR). J Biol Chem. 2013 Jun 28;288(26):18707-15.

[16] Luu W, Hart-Smith G, Sharpe LJ, Brown AJ. The terminal enzymes of cholesterol synthesis, DHCR24 and DHCR7, interact physically and functionally. J Lipid Res. 2015 Apr;56(4):888-97.
[17] Valenza M, Carroll JB, Leoni V, Bertram LN, Bjorkhem I, Singaraja RR, Di Donato S, Lutjohann D, Hayden MR, Cattaneo E. Cholesterol biosynthesis pathway is disturbed in YAC128 mice and is modulated by huntingtin mutation. Hum Mol Genet. 2007 Sep 15;16(18):2187-98.
[18] Lutjohann D, Breuer O, Ahlborg G, Nennesmo I, Siden I, Diczfalusy U, Bjorkhem I. Cholesterol homeostasis in human brain: Evidence for an age-dependent flux of 24S-hydroxycholesterol from the brain into the circulation. Proc Natl Acad Sci U S A. 1996;93:9799-9804.
[19] Bjorkhem I, Lutjohann D, Diczfalusy U, Stahle L, Ahlborg G, Wahren J. Cholesterol homeostasis in human brain: turnover of 24S-hydroxycholesterol and evidence for a cerebral origin of most of this oxysterol in the circulation. J Lipid Res. 1998 Aug;39(8):1594-1600.
[20] Lund EG, Guileyardo JM, Russell DW. cDNA cloning of cholesterol 24-hydroxylase, a mediator of cholesterol homeostasis in the brain. Proc Natl Acad Sci U S A. 1999 Jun 22;96(13):7238-43.
[21] Leoni V, Mariotti C, Tabrizi SJ, Valenza M, Wild EJ, Henley SMD, Hobbs NZ, Mandelli ML, Grisoli M, Bjorkhem I, Cattaneo E, Di Donato S. Plasma 24S-hydroxycholesterol and caudate MRI in pre-manifest and early Huntingtons disease. Brain. 2008 Nov;131:2851-2859.
[22] Leoni V, Long JD, Mills JA, Di Donato S, Paulsen JS, group P-Hs. Plasma 24S-hydroxycholesterol correlation with markers of Huntington disease progression. Neurobiol Dis. 2013 Jul;55:37-43.
[23] Kolsch H, Lutjohann D, Ludwig M, Schulte A, Ptok U, Jessen F, von Bergmann K, Rao ML, Maier W, Heun R. Polymorphism in the cholesterol 24S-hydroxylase gene is associated with Alzheimer's disease. Mol Psychiatry. 2002;7(8):899-902.
[24] Brown J, 3rd, Theisler C, Silberman S, Magnuson D, Gottardi-Littell N, Lee JM, Yager D, Crowley J, Sambamurti K, Rahman MM, Reiss AB, Eckman CB, Wolozin B. Differential expression of cholesterol hydroxylases in Alzheimer's disease. J Biol Chem. 2004 Aug 13;279(33):34674-81.
[25] Papassotiropoulos A, Streffer JR, Tsolaki M, Schmid S, Thal D, Nicosia F, Iakovidou V, Maddalena A, Lutjohann D, Ghebremedhin E, Hegi T, Pasch T, Traxler M, Bruhl A, Benussi L, Binetti G, Braak H, Nitsch RM, Hock C. Increased brain beta-amyloid load, phosphorylated tau, and risk of Alzheimer disease associated with an intronic CYP46 polymorphism. Arch Neurol. 2003 Jan;60(1):29-35.
[26] Tian G, Kong Q, Lai L, Ray-Chaudhury A, Lin CL. Increased expression of cholesterol 24S-hydroxylase results in disruption of glial glutamate transporter EAAT2 association with lipid rafts: a potential role in Alzheimer's disease. J Neurochem. 2010 May;113(4):978-89.
[27] Martin KO, Budai K, Javitt NB. Cholesterol and 27-hydroxycholesterol 7 alpha-hydroxylation: evidence for two different enzymes. J Lipid Res [Research Support, U.S. Gov't, P.H.S.]. 1993 Apr;34(4):581-8.
[28] Lund E, Andersson O, Zhang J, Babiker A, Ahlborg G, Diczfalusy U, Einarsson K, Sjovall J, Bjorkhem I. Importance of a novel oxidative mechanism for elimination of intracellular cholesterol in humans. Arteriosclerosis, thrombosis, and vascular biology [Research Support, Non-U.S. Gov't]. 1996 Feb;16(2):208-12.

[29] Heverin M, Meaney S, Lutjohann D, Diczfalusy U, Wahren J, Bjorkhem I. Crossing the barrier: net flux of 27-hydroxycholesterol into the human brain. J Lipid Res. 2005 May;46(5):1047-1052.

[30] Meaney S, Heverin M, Panzenboeck U, Ekstrom L, Axelsson M, Andersson U, Diczfalusy U, Pikuleva I, Wahren J, Sattler W, Bjorkhem I. Novel route for elimination of brain oxysterols across the blood-brain barrier: conversion into 7alpha-hydroxy-3-oxo-4-cholestenoic acid. J Lipid Res. 2007 Apr;48(4):944-51.

[31] Shafaati M, Marutle A, Pettersson H, Lovgren-Sandblom A, Olin M, Pikuleva I, Winblad B, Nordberg A, Bjorkhem I. Marked accumulation of 27-hydroxycholesterol in the brains of Alzheimer's patients with the Swedish APP 670/671 mutation. J Lipid Res. 2011 May;52(5):1004-10.

[32] Heverin M, Bogdanovic N, Lutjohann D, Bayer T, Pikuleva I, Bretillon L, Diczfalusy U, Winblad B, Bjorkhem I. Changes in the levels of cerebral and extracerebral sterols in the brain of patients with Alzheimer's disease. J Lipid Res. 2004 Jan;45(1):186-93.

[33] Subbarao KV, Richardson JS, Ang LC. Autopsy samples of Alzheimer's cortex show increased peroxidation in vitro. J Neurochem. 1990 Jul;55(1):342-5.

[34] Cheng D, Jenner AM, Shui G, Cheong WF, Mitchell TW, Nealon JR, Kim WS, McCann H, Wenk MR, Halliday GM, Garner B. Lipid pathway alterations in Parkinson's disease primary visual cortex. PLoS One. 2011;6(2):e17299.

[35] Jenner A, Ren M, Rajendran R, Ning P, Huat BT, Watt F, Halliwell B. Zinc supplementation inhibits lipid peroxidation and the development of atherosclerosis in rabbits fed a high cholesterol diet. Free Radic Biol Med. 2007 Feb 15;42(4):559-66.

[36] Iuliano L, Micheletta F, Natoli S, Corradini SG, Iappelli M, Elisei W, Giovannelli L, Violi F, Diczfalusy U. Measurement of oxysterols and alpha-tocopherol in plasma and tissue samples as indices of oxidant stress status. Anal Biochem. 2003 Jan 15;312(2):217-223.

[37] Iuliano L, Monticolo R, Straface G, Zullo S, Galli F, Boaz M, Quattrucci S. Association of cholesterol oxidation and abnormalities in fatty acid metabolism in cystic fibrosis. Am J Clin Nutr. 2009 Sep;90(3):477-84.

[38] Rodriguez IR, Fliesler SJ. Photodamage generates 7-keto- and 7-hydroxycholesterol in the rat retina via a free radical-mediated mechanism. Photochem Photobiol. 2009 Sep-Oct;85(5):1116-25.

[39] Mangiarini L, Sathasivam K, Seller M, Cozens B, Harper A, Hetherington C, Lawton M, Trottier Y, Lehrach H, Davies SW, Bates GP. Exon 1 of the HD gene with an expanded CAG repeat is sufficient to cause a progressive neurological phenotype in transgenic mice. Cell. 1996 Nov 1;87(3):493-506.

[40] Mazarakis NK, Cybulska-Klosowicz A, Grote H, Pang T, Van Dellen A, Kossut M, Blakemore C, Hannan AJ. Deficits in experience-dependent cortical plasticity and sensory-discrimination learning in presymptomatic Huntington's disease mice. J Neurosci. 2005 Mar 23;25(12):3059-66.

[41] Nithianantharajah J, Barkus C, Murphy M, Hannan AJ. Gene-environment interactions modulating cognitive function and molecular correlates of synaptic plasticity in Huntington's disease transgenic mice. Neurobiol Dis. 2008 Mar;29(3):490-504.

[42] Grote HE, Bull ND, Howard ML, van Dellen A, Blakemore C, Bartlett PF, Hannan AJ. Cognitive disorders and neurogenesis deficits in Huntington's disease mice are rescued by fluoxetine. Eur J Neurosci. 2005 Oct;22(8):2081-8.

[43] Pang TY, Du X, Zajac MS, Howard ML, Hannan AJ. Altered serotonin receptor expression is associated with depression-related behavior in the R6/1 transgenic mouse model of Huntington's disease. Hum Mol Genet. 2009 Feb 15;18(4):753-66.

[44] Zhang Y, Appelkvist EL, Kristensson K, Dallner G. The lipid compositions of different regions of rat brain during development and aging. Neurobiol Aging. 1996 Nov-Dec;17(6):869-75.
[45] Dietschy JM, Turley SD. Thematic review series: brain Lipids. Cholesterol metabolism in the central nervous system during early development and in the mature animal. J Lipid Res. 2004 Aug;45(8):1375-97.
[46] Bartzokis G, Lu PH, Tishler TA, Fong SM, Oluwadara B, Finn JP, Huang D, Bordelon Y, Mintz J, Perlman S. Myelin breakdown and iron changes in Huntington's disease: pathogenesis and treatment implications. Neurochem Res. 2007 Oct;32(10):1655-64.
[47] Thelen KM, Falkai P, Bayer TA, Lutjohann D. Cholesterol synthesis rate in human hippocampus declines with aging. Neurosci Lett. 2006 Jul 31;403(1-2):15-9.
[48] Marullo M, Valenza M, Leoni V, Caccia C, Scarlatti C, De Mario A, Zuccato C, Di Donato S, Carafoli E, Cattaneo E. Pitfalls in the detection of cholesterol in Huntington's disease models. PLoS Curr. 2012;4:e505886e9a1968.
[49] Lodi R, Schapira AH, Manners D, Styles P, Wood NW, Taylor DJ, Warner TT. Abnormal in vivo skeletal muscle energy metabolism in Huntington's disease and dentatorubropallidoluysian atrophy. Ann Neurol. 2000 Jul;48(1):72-6.
[50] Chen CM, Wu YR, Cheng ML, Liu JL, Lee YM, Lee PW, Soong BW, Chiu DT. Increased oxidative damage and mitochondrial abnormalities in the peripheral blood of Huntington's disease patients. Biochem Biophys Res Commun. 2007 Jul 27;359(2):335-40.
[51] Perez-Severiano F, Rios C, Segovia J. Striatal oxidative damage parallels the expression of a neurological phenotype in mice transgenic for the mutation of Huntington's disease. Brain Res. 2000 Apr 17;862(1-2):234-7.
[52] Morales LM, Estevez J, Suarez H, Villalobos R, Chacin de Bonilla L, Bonilla E. Nutritional evaluation of Huntington disease patients. The American journal of clinical nutrition. 1989 Jul;50(1):145-50.
[53] Sanberg PR, Fibiger HC, Mark RF. Body weight and dietary factors in Huntington's disease patients compared with matched controls. The Medical journal of Australia [Comparative Study]. 1981 Apr 18;1(8):407-9.
[54] Clifford JJ, Drago J, Natoli AL, Wong JY, Kinsella A, Waddington JL, Vaddadi KS. Essential fatty acids given from conception prevent topographies of motor deficit in a transgenic model of Huntington's disease. Neuroscience [Research Support, Non-U.S. Gov't]. 2002;109(1):81-8.
[55] Naver B, Stub C, Moller M, Fenger K, Hansen AK, Hasholt L, Sorensen SA. Molecular and behavioral analysis of the R6/1 Huntington's disease transgenic mouse. Neuroscience. 2003;122(4):1049-57.

Figure legends

Fig. 1 Simplified pathway showing cholesterol synthesis, metabolism and free radical oxidation relevant to this study. The lower cholesterol synthetic (downstream of squalene) pathway is branched into the Kandutsch-Russell pathway (via lathosterol) and Bloch pathway (via desmosterol). Major metabolic pathways of cholesterol involve the enzymatic hydroxylation of cholesterol by; cholesterol 24-hydroxylase (CYP46A1) to form 24-hydroxycholesterol (24-OHC), and cholesterol 27-hydroxylase (CYP27A1) to form 27-hydroxycholesterol (27-OHC). Free radical mediated oxidation of cholesterol can also occur. Reactive oxygen species (ROS) form 7-Ketocholesterol and 7β-hydroxycholesterol. The position of delta(24)-sterol reductase (DHCR24), a cholesterol synthetic enzyme is also shown. Broken lines indicate intermediates that have not been shown in this simplified scheme

Fig. 2 Progression of the physical phenotype in male and female R6/1 mice. (**A**) R6/1 mice had significantly reduced body weight compared to WT over the course of the study ($p < 0.0001$). The R6/1 weight loss phenotype is more severe in male mice compared to females. Male R6/1 mice begin to lose weight after 16 weeks compared to 19 weeks in females. The rate of weight gain prior to weight loss was significantly slower in R6/1 females compared to WT ($p = 0.00012$) while no difference was observed in male mice. (**B**) R6/1 mice develop a phenotype where the hind paws are clasped to the body when suspended by the tail. Male R6/1 mice exhibited the phenotype prior to females; the occurrence of the phenotype increased in the population during ageing with 60% of the R6/1 mice showing a positive clasping phenotype by 28 weeks. A small proportion of WT mice appeared to exhibit a half clasp phenotype during the course of the study. (**C**) The motor performance of mice was tested throughout the study and a progressive decline was found in the ability of R6/1 male

and female mice to run on an accelerating rod when compared to WT ($p = 0.0016$ and 0.0004 respectively). No difference between male and female mice with the same genotype was detected. Closed circles represent R6/1, open circles represent WT. n = 5 per group. Error bars represent ± SEM

Fig. 3 Brain mass of R6/1 mice during disease progression. Brain mass was significantly reduced in both R6/1 male and female mice compared to WT at later stages. The difference between WT and R6/1 male mice was highly significant at 20, 24 and 28 weeks. A significant difference between R6/1 and WT female mice was detected at 12 and 20 weeks, becoming highly significant at 24 and 28 weeks. The brain mass was measured from mice sacrificed at lipid analysis time points; each point represents 5-7 mice. Closed circles represent R6/1, open circles represent WT. Error bars represent ± SEM. 2-way ANOVA Bonferroni post-test *$p < 0.05$ ***$p < 0.0001$

Fig. 4 Cholesterol synthetic precursor levels in striatum tissue of R6/1 and WT littermates. Extracted sterols were quantified using heavy isotope mass dilution GC-MS/MS. (**A**) Lathosterol, (**B**) lanosterol and (**C**) zymosterol levels were significantly reduced early in the R6/1 mice compared to WT. (**D**) 24,25 dihydro lanosterol showed a trend to be decreased in R6/1 mice however there was no significant difference between WT and R6/1 at any time-point. Lanosterol, lathosterol, zymosterol and 24,25 dihydro lanosterol decreased over time in both R6/1 and WT mice ($p < 0.01$). (**E**) Desmosterol did not significantly decline in R6/1 mice, and was significantly elevated at 20 and 28 weeks compared to control. (**F**) 7-Dehydrocholesterol did not significantly decline in R6/1 mice and no significant differences were detected between R6/1 and WT at any time point. Each data point represents combined results from male and female mice, n = 10-13 per group. Closed circles represent R6/1, open circles represent WT. Error bars represent ± SEM. 2-way ANOVA Bonferroni post-test *$p < 0.05$ **$p < 0.01$ ***$p < 0.0001$. t-test $^{\Psi}p < 0.05$

Fig. 5 Cholesterol synthetic precursor levels in cortex tissue of R6/1 and WT littermates. Extracted sterols were quantified using heavy isotope mass dilution GC-MS/MS. (**A**) Lathosterol and (**B**) lanosterol levels were significantly reduced early in R6/1 mice compared to WT. (**C**) Zymosterol was significantly reduced in R6/1 at the end time point. (**D**) 24,25 dihydro lanosterol had a trend to be reduced however there was no significant difference between WT and R6/1 at any time-point. Zymosterol, lanosterol and 24,25 dihydro lanosterol decreased in R6/1 over time while WT levels remained unchanged ($p < 0.01$). Lathosterol levels decreased both in R6/1 and WT at a similar rate. (**E**) Desmosterol levels did not change over time in R6/1 or WT mice, however desmosterol was elevated in R6/1 mice at 28 weeks. (**F**) 7-Dehydrocholesterol did not significantly decline in R6/1 mice and no significant differences were detected between R6/1 and WT at any time point. Each data point represents combined results from male and female mice, n = 10-13 per group. Closed circles represent R6/1, open circles represent WT. Error bars represent ± SEM. 2-way ANOVA Bonferroni post-test *$p < 0.05$ **$p < 0.01$ ***$p < 0.0001$. t-test $^{\Psi}p < 0.05$

Fig. 6 The level of cholesterol and cholesterol metabolites in striatum and cortex tissue of R6/1 and WT littermates. Extracted sterols were quantified using heavy isotope mass dilution GC-MS/MS. 24(S)-Hydroxycholesterol was significantly reduced in striatum of R6/1 mice compared to WT at the end stage of the study. A significant reduction in 27-hydroxycholesterol levels was detected at 12, 20, 24 and 28 weeks in the R6/1 striatum. An effect of genotype on cortical levels of 24-hydroxycholesterol and 27-hydroxycholesterol was not detected at any time point. Cholesterol levels were unaltered between R6/1 and WT mice in both striatum and cortex at all time-points examined. A significant increase in 24-hydroxycholesterol and cholesterol levels over time was detected in both regions ($p < 0.01$ and $p < 0.05$ respectively). Each data point represents combined results from male and female

mice, n = 10-13 per group. Closed circles represent R6/1, open circles represent WT. Error bars represent ± SEM. Bonferroni post-test *p < 0.05 **p < 0.01

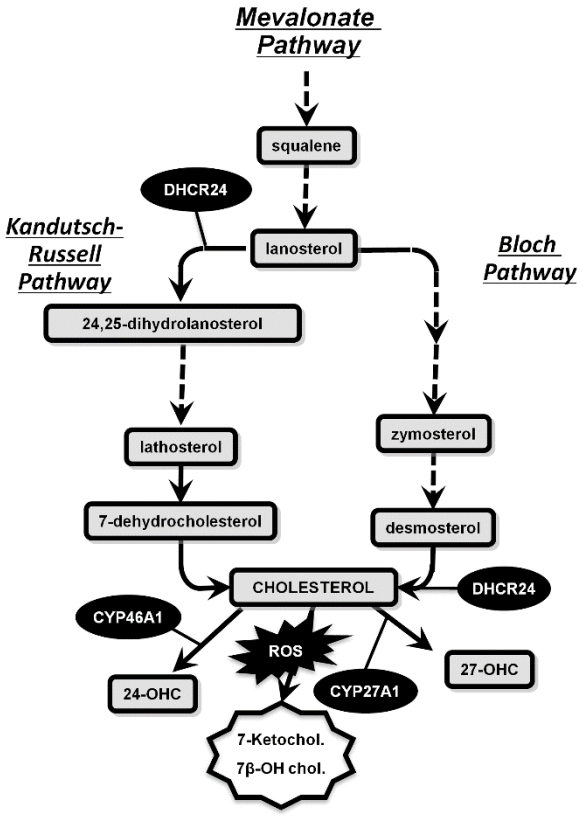

Fig. 1

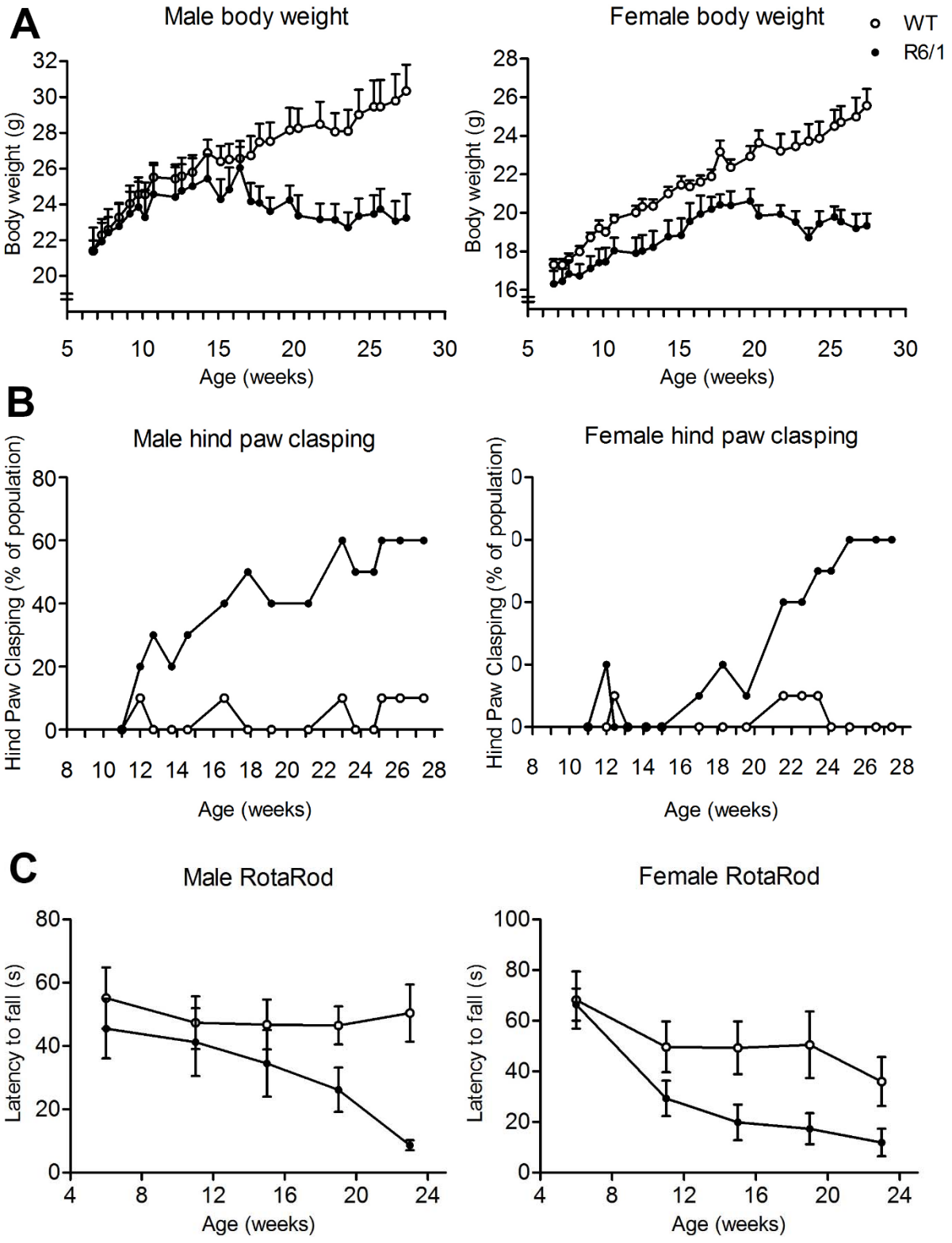
A
Male body weight
Female body weight
WT
R6/1
Body weight (g)
Age (weeks)
B
Male hind paw clasping
Female hind paw clasping
Hind Paw Clasping (% of population)
Age (weeks)
C
Male RotaRod
Female RotaRod
Latency to fall (s)
Age (weeks)

Fig. 2

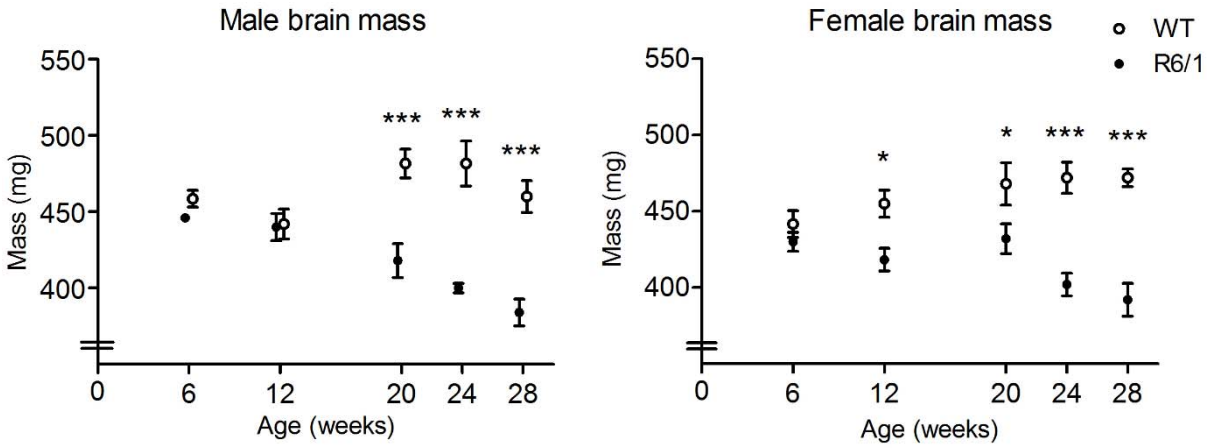
Male brain mass
Female brain mass
WT
R6/1
Mass (mg)
550
500
450
400
0
6
12
20
24
28
Age (weeks)
***
*

Fig. 3

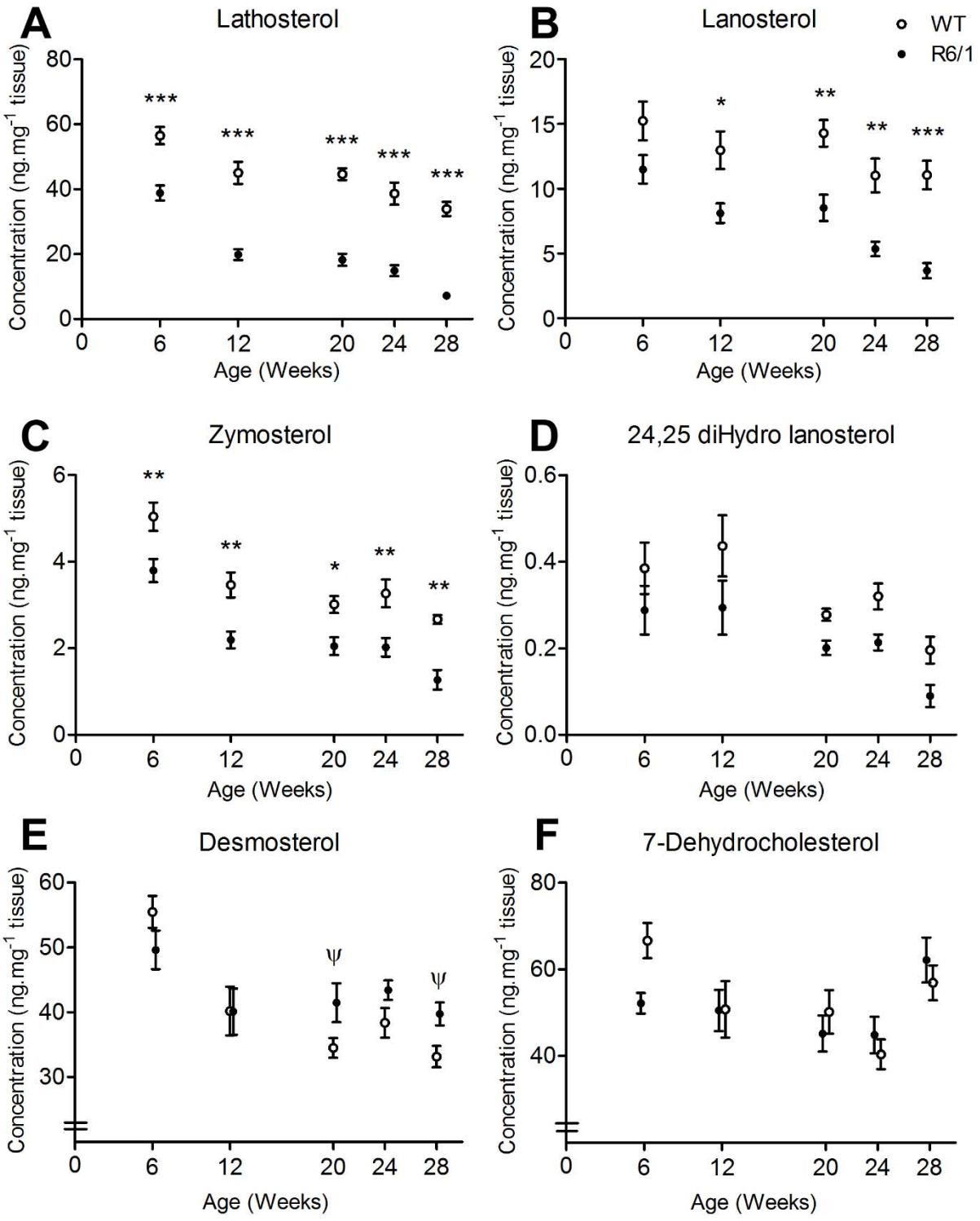
A
Lathosterol
B
Lanosterol
WT
R6/1
C
Zymosterol
D
24,25 diHydro lanosterol
E
Desmosterol
F
7-Dehydrocholesterol
Concentration (ng.mg-1 tissue)
Age (Weeks)
0
6
12
20
24
28
***
**
*
ψ

Fig. 4

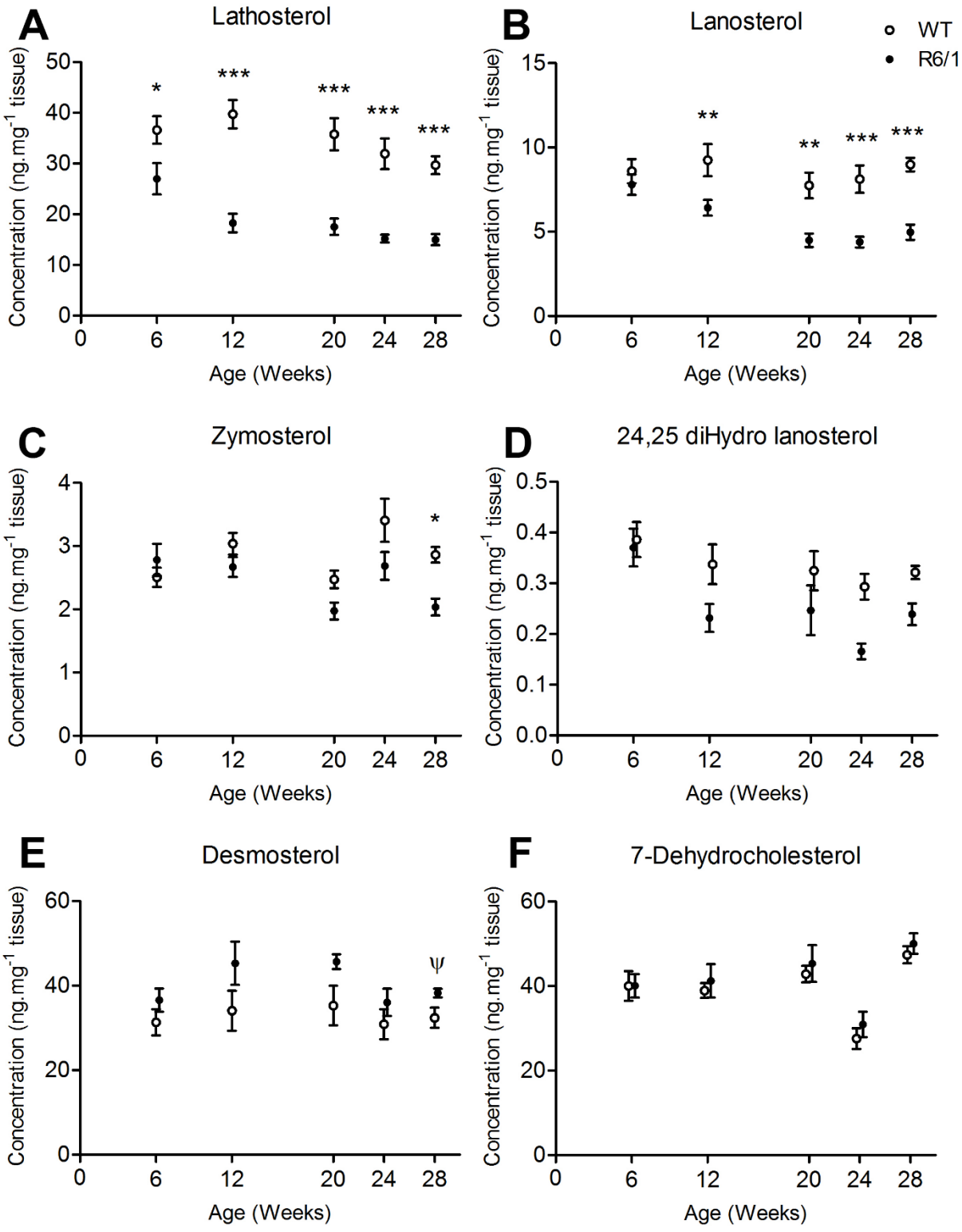
A
Lathosterol
Concentration (ng.mg-1 tissue)
Age (Weeks)
B
Lanosterol
WT
R6/1
C
Zymosterol
D
24,25 diHydro lanosterol
E
Desmosterol
F
7-Dehydrocholesterol

Fig. 5

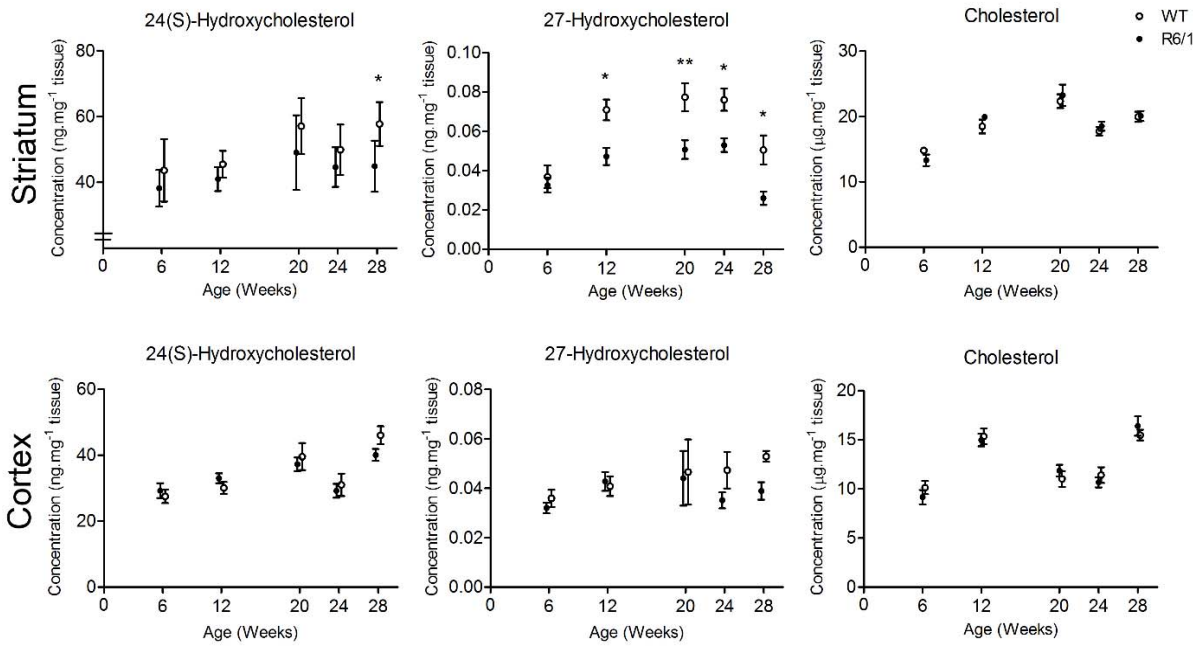
Striatum
Cortex
24(S)-Hydroxycholesterol
27-Hydroxycholesterol
Cholesterol
WT
R6/1
Concentration (ng.mg-1 tissue)
Concentration (µg.mg-1 tissue)
Age (Weeks)
0
6
12
20
24
28

Fig. 6

Supplemental Table 1 **Absolute values of sterols in male R6/1 and WT cortex and striatum.** GC-MS/MS was used to analyse lipids extracted from mouse brain tissue at various stages of the disease. Values represent ng/mg tissue ± SD.

		Male									
		6 week		12 week		20 week		24 week		28 week	
		WT	HD	WT	HD	WT	HD	WT	HD	WT	HD
Striatum	Lathosterol	54.8 ± 5.6	41.7 ± 6.7	43.2 ± 6.2	20.0 ± 4.8	41.6 ± 5.7	17.8 ± 6.1	43.8 ± 10.7	12.6 ± 3.5	31.4 ± 6.0	8.7 ± 2.7
	Lanosterol	13.6 ± 3.8	13.1 ± 3.6	10.8 ± 1.7	8.3 ± 2.5	13.6 ± 2.7	8.7 ± 3.4	12.2 ± 4.0	4.5 ± 1.3	8.9 ± 2.5*	4.7 ± 1.7
	Zymosterol	5.0 ± 1.3	4.0 ± 0.9	3.2 ± 0.4	2.2 ± 0.4	2.9 ± 0.63	2.2 ± 0.83	3.5 ± 0.88	1.8 ± 0.36	2.7 ± 0.4	1.5 ± 0.6
	24,25 diH lan.	0.34 ± 0.22	0.39 ± 0.19	0.33 ± 0.09	0.24 ± 0.18	0.26 ± 0.05	0.19 ± 0.06	0.31 ± 0.07	0.20 ± 0.07	0.19 ± 0.09	0.13 ± 0.08
	Desmosterol	57.0 ± 9.1	57.7 ± 3.8*	31.1 ± 9.6*	39.7 ± 17.2	35.8 ± 5.1	41.7 ± 12.6	39.8 ± 8.1	42.0 ± 4.6	33.0 ± 5.9	40.1 ± 7.3
	7-DHC	63.0 ± 15.9	59.0 ± 4.9*	43.5 ± 22.4	48.4 ± 21.8	54.3 ± 16.8	46.7 ± 14.6	37.9 ± 7.0	42.5 ± 12.6	57.3 ± 15.3	68.7 ± 15.3
	24-OHC	48.5 ± 8.7*	42.3 ± 4.8*	46.8 ± 4.1	39.7 ± 4.1	57.6 ± 11.2	48.6 ± 15.1	53.3 ± 8.5	45.5 ± 5.2	53.7 ± 3.4*	40.5 ± 8.3
	27-OHC	0.039 ± 0.02	0.034 ± 0.01	0.078 ± 0.02	0.051 ± 0.01	0.083 ± 0.03	0.052 ± 0.02	0.075 ± 0.012	0.051 ± 0.014	0.043 ± 0.02	0.024 ± 0.01
	7-KC	0.67 ± 0.26	0.66 ± 0.29*	0.65 ± 0.18	0.65 ± 0.15	0.30 ± 0.003	0.28 ± 0.009	0.58 ± 0.19	0.52 ± 0.11	0.65 ± 0.29	0.41 ± 0.17
	7β-OHC	0.36 ± 0.12	0.36 ± 0.17	0.45 ± 0.19	0.54 ± 0.27	0.26 ± 0.005	0.26 ± 0.010	0.21 ± 0.06	0.22 ± 0.06	0.28 ± 0.13	0.23 ± 0.11
	Cholesterol[a]	15.1 ± 1.1	13.6 ± 4.3	17.8 ± 3.1	19.9 ± 1.4	21.5 ± 2.6	21.7 ± 6.0	19.1 ± 1.8*	18.9 ± 1.9	19.2 ± 3.0	19.8 ± 3.2
Cortex	Lathosterol	33.5 ± 8.7	27.7 ± 11.2	34.7 ± 14.8	14.8 ± 4.1	34.5 ± 10.8	19.5 ± 3.1	32.1 ± 11.9	14.8 ± 3.3	28.8 ± 5.5	14.6 ± 3.1
	Lanosterol	7.9 ± 1.4	8.3 ± 2.9	7.9 ± 2.7	5.7 ± 1.4	12.3 ± 4.7	7.4 ± 1.7	6.7 ± 2.3	4.2 ± 1.2	8.4 ± 1.3	4.6 ± 1.2
	Zymosterol	2.4 ± 0.66	2.9 ± 1.1	2.9 ± 0.6	2.5 ± 0.6	2.7 ± 0.6	2.0 ± 0.3	3.0 ± 1.2	2.7 ± 0.85	2.9 ± 0.30	2.0 ± 0.42
	24,25 diH lan.	0.33 ± 0.06	0.40 ± 0.17	0.32 ± 0.11	0.22 ± 0.07	0.37 ± 0.18	0.32 ± 0.17	0.22 ± 0.07	0.14 ± 0.04	0.32 ± 0.03	0.25 ± 0.09
	Desmosterol	32.8 ± 14.9	36.8 ± 9.2	34.6 ± 16.3	42.4 ± 16.4	41.9 ± 12.9*	47.3 ± 7.3	27.0 ± 9.5	33.1 ± 9.4	32.0 ± 8.1	38.0 ± 2.1
	7-DHC	39.5 ± 17.2	41.2 ± 9.9	39.9 ± 6.0	40.5 ± 12.0	44.1 ± 6.4	44.5 ± 13.2	31.0 ± 7.0	30.6 ± 9.9	45.6 ± 7.4	49.7 ± 6.2
	24-OHC	28.4 ± 9.5	27.3 ± 7.5	29.7 ± 7.8	33.5 ± 7.5	40.3 ± 7.7	37.4 ± 9.0	23.6 ± 5.7*	26.2 ± 6.7	46.3 ± 6.7	42.4 ± 6.7
	27-OHC	0.038 ± 0.02	0.030 ± 0.008	0.037 ± 0.01	0.038 ± 0.01	0.099 ± 0.06*	0.071 ± 0.03*	0.034 ± 0.007	0.032 ± 0.011	0.051 ± 0.008	0.044 ± 0.01
	7-KC	0.27 ± 0.12*	0.32 ± 0.13	0.51 ± 0.04	0.50 ± 0.09	0.37 ± 0.11	0.58 ± 0.16	0.31 ± 0.08	0.22 ± 0.04*	0.86 ± 0.50	1.0 ± 1.05
	7β-OHC	0.14 ± 0.07	0.18 ± 0.10	0.40 ± 0.11	0.35 ± 0.14	0.12 ± 0.03	0.16 ± 0.12	0.12 ± 0.02	0.15 ± 0.07	0.43 ± 0.30	0.20 ± 0.09
	Cholesterol[a]	9.5 ± 2.6	9.2 ± 2.8	13.8 ± 1.8	14.6 ± 2.0	10.5 ± 2.0	12.8 ± 1.4	11.0 ± 2.1	10.4 ± 1.9	15.4 ± 1.9	17.6 ± 2.9

24, 25 diH lan. = 24, 25 dihydro lanosterol; 7-DHC = 7-dehydrocholesterol; 24-OHC = 24(S)-hydroxycholesterol; 27-OHC = 27-hydroxycholesterol; 7-KC = 7-ketocholesterol; 7β-OHC = 7β-hydroxycholesterol. [a]Values expressed as µg/mg tissue. *Values identified to be significantly different between male and female of the same genotype, t-test $p < 0.05$.

Supplemental Table 2 **Absolute values of sterols in female R6/1 and WT cortex and striatum.** GC-MS/MS was used to analyse lipids extracted from mouse brain tissue at various stages of the disease. Values represent ng/mg tissue ± SD.

		Female									
		6 week		12 week		20 week		24 week		28 week	
		WT	HD	WT	HD	WT	HD	WT	HD	WT	HD
Striatum	Lathosterol	58.5 ± 13.7	36.4 ± 8.3	46.6 ± 14.8	19.7 ± 6.6	48.3 ± 4.1	18.7 ± 6.4	33.5 ± 8.9	17.7 ± 6.8	36.4 ± 7.8	5.7 ± 1.9
	Lanosterol	17.1 ± 6.7	10.2 ± 3.3	14.8 ± 5.9	7.9 ± 2.8	15.2 ± 4.3	8.3 ± 3.4	9.8 ± 4.3	6.4 ± 1.9	13.3 ± 3.0*	2.7 ± 1.4
	Zymosterol	5.1 ± 1.2	3.6 ± 0.93	3.6 ± 1.3	2.1 ± 0.8	3.1 ± 0.74	1.9 ± 0.43	3.0 ± 1.2	2.3 ± 0.98	2.7 ± 0.3	1.1 ± 0.8
	24,25 diH lan.	0.44 ± 0.22	0.20 ± 0.14	0.51 ± 0.26	0.33 ± 0.20	0.30 ± 0.03	0.21 ± 0.05	0.33 ± 0.012	0.23 ± 0.05	0.21 ± 0.12	0.04 ± 0.03
	Desmosterol	53.7 ± 9.1	42.9 ± 8.2*	47.8 ± 9.1*	40.4 ± 6.8	33.0 ± 5.0	41.3 ± 6.5	37.0 ± 6.7	45.1 ± 5.4	33.4 ± 5.1	39.4 ± 4.0
	7-DHC	70.9 ± 13.2	46.9 ± 5.3*	56.8 ± 21.0	52.3 ± 10.6	45.3 ± 16.8	44.0 ± 13.2	42.9 ± 14.0	47.7 ± 16.6	56.5 ± 10.8	55.4 ± 16.1
	24-OHC	38.1 ± 7.5*	34.8 ± 3.6*	45.1 ± 4.2	43.1 ± 3.1	56.5 ± 4.7	49.5 ± 7.9	46.5 ± 5.6	43.6 ± 7.4	61.9 ± 6.8*	49.3 ± 4.6
	27-OHC	0.034 ± 0.02	0.030 ± 0.01	0.067 ± 0.01	0.046 ± 0.02	0.071 ±	0.049 ± 0.12	0.078 ± 0.02	0.056 ± 0.008	0.058 ± 0.02	0.028 ± 0.009
	7-KC	0.84 ± 0.57	0.33 ± 0.06*	0.60 ± 0.21	0.70 ± 0.16	0.33 ± 0.008	0.32 ± 0.008	0.49 ± 0.18	0.57 ± 0.19	0.38 ± 0.05	0.57 ± 0.19
	7β-OHC	0.35 ± 0.28	0.20 ± 0.05	0.44 ± 0.12	0.57 ± 0.18	0.23 ± 0.004	0.23 ± 0.005	0.20 ± 0.07	0.24 ± 0.06	0.20 ± 0.07	0.25 ± 0.13
	Cholesterol[a]	14.5 ± 1.5	13.1 ± 1.4	19.5 ± 3.5	20.3 ± 1.5	23.3 ± 4.4	24.8 ± 4.1	16.4 ± 1.5*	18.0 ± 2.8	20.67 ± 1.7	20.4 ± 1.6
Cortex	Lathosterol	40.2 ± 10.3	26.3 ± 10.4	43.9 ± 9.9	21.2 ± 6.1	41.6 ± 8.8	15.5 ± 6.3	31.8 ± 7.9	15.6 ± 1.7	30.6 ± 6.1	15.3 ± 4.0
	Lanosterol	9.4 ± 3.5	7.4 ± 1.1	10.4 ± 3.3	7.0 ± 1.5	10.9 ± 2.6	5.5 ± 1.6	9.5 ± 2.2	4.6 ± 0.99	9.6 ± 0.94	5.3 ± 1.7
	Zymosterol	2.6 ± 0.44	2.7 ± 0.69	3.2 ± 0.6	2.8 ± 0.4	2.4 ± 0.5	1.9 ± 0.6	3.8 ± 0.94	2.7 ± 0.65	2.8 ± 0.50	2.0 ± 0.48
	24,25 diH lan.	0.45 ± 0.16	0.35 ± 0.08	0.35 ± 0.15	0.24 ± 0.11	0.32 ± 0.08	0.17 ± 0.11	0.27 ± 0.07	0.14 ± 0.05	0.32 ± 0.05	0.23 ± 0.04
	Desmosterol	29.6 ± 5.1	36.8 ± 10.0	33.6 ± 16.7	47.6 ± 18.6	26.1 ± 7.3*	44.0 ± 2.9	34.8 ± 12.5	39.5 ± 12.2	32.8 ± 7.9	38.5 ± 4.3
	7-DHC	40.6 ± 4.9	39.1 ± 9.4	38.1 ± 6.1	41.8 ± 15.1	42.5 ± 7.3	46.0 ± 16.6	24.1 ± 7.5	31.3 ± 11.3	49.2 ± 5.5	50.4 ± 9.6
	24-OHC	26.6 ± 4.8	30.9 ± 7.6	30.4 ± 4.8	32.6 ± 2.5	38.7 ± 17.4	37.2 ± 3.6	38.5 ± 9.5*	32.9 ± 5.8	45.8 ± 10.9	37.8 ± 3.7
	27-OHC	0.034 ± 0.008	0.033 ± 0.008	0.044 ± 0.02	0.047 ± 0.01	0.021 ± 0.006*	0.017 ± 0.005*	0.060 ± 0.03	0.039 ± 0.01	0.055 ± 0.007	0.033 ± 0.007
	7-KC	0.49 ± 0.18*	0.33 ± 0.11	0.49 ± 0.17	0.46 ± 0.18	0.46 ± 0.22	0.51 ± 0.25	0.33 ± 0.10	0.35 ± 0.11*	0.91 ± 0.62	0.78 ± 0.68
	7β-OHC	0.24 ± 0.12	0.22 ± 0.14	0.37 ± 0.17	0.37 ± 0.12	0.15 ± 0.06	0.16 ± 0.04	0.11 ± 0.02	0.18 ± 0.06	0.35 ± 0.35	0.23 ± 0.11
	Cholesterol[a]	10.9 ± 2.1	9.1 ± 2.4	16.6 ± 2.7	15.3 ± 2.3	12.2 ± 2.9	10.9 ± 1.9	11.8 ± 3.04	10.9 ± 1.7	15.5 ± 1.8	15.2 ± 3.1

24, 25 diH lan. = 24, 25 dihydro lanosterol; 7-DHC = 7-dehydrocholesterol; 24-OHC = 24(S)-hydroxycholesterol; 27-OHC = 27-hydroxycholesterol; 7-KC = 7-ketocholesterol; 7β-OHC = 7β-hydroxycholesterol. [a]Values expressed as μg/mg tissue. *Values identified to be significantly different between male and female of the same genotype, t-test $p < 0.05$.

Supplemental Table 3 **Absolute values of sterols in combined sexes R6/1 and WT cortex and striatum.** GC-MS/MS was used to analyse lipids extracted from mouse brain tissue at various stages of the disease. Values represent ng/mg tissue ± SD.

		Combined									
		6 week		12 week		20 week		24 week		28 week	
		WT	HD	WT	HD	WT	HD	WT	HD	WT	HD
Striatum	Lathosterol	56.5 ± 9.6	38.8 ± 7.8	45.0 ± 11.3	19.8 ± 5.6	44.6 ± 6.0	18.3 ± 5.9	38.6 ± 10.7	14.9 ± 5.6	33.9 ± 7.0	7.2 ± 2.7
	Lanosterol	15.2 ± 5.4	11.5 ± 3.6	12.9 ± 4.8	8.1 ± 2.5	14.3 ± 3.4	8.5 ± 3.2	11.0 ± 4.1	5.4 ± 1.9	11.1 ± 3.5	3.7 ± 1.8
	Zymosterol	5.0 ± 1.2	3.8 ± 0.88	3.5 ± 0.9	2.2 ± 0.6	3.0 ± 0.65	2.0 ± 0.65	3.7 ± 1.0	2.0 ± 0.71	2.7 ± 0.33	1.3 ± 0.72
	24,25 diH lan.	0.38 ± 0.21	0.29 ± 0.19	0.44 ± 0.22	0.29 ± 0.19	0.28 ± 0.05	0.20 ± 0.05	0.32 ± 0.09	0.21 ± 0.06	0.20 ± 0.10	0.090 ±
	Desmosterol	55.5 ± 8.9	49.6 ± 9.9	40.2 ± 12.4	40.1 ± 11.9	34.5 ± 5.0	41.5 ± 9.5	38.4 ± 7.2	43.4 ± 5.0	33.2 ± 5.2	39.8 ± 5.6
	7-DHC	66.6 ± 14.7	52.2 ± 7.8	50.8 ± 21.6	50.5 ± 15.8	50.2 ± 16.6	45.2 ± 13.2	40.4 ± 10.8	44.9 ± 14.0	56.9 ± 12.8	62.2 ± 16.4
	24-OHC	43.7 ± 9.5	38.2 ± 5.6	45.5 ± 4.1	41.0 ± 3.6	57.1 ± 8.5	49.1 ± 11.4	49.9 ± 7.7	44.6 ± 6.0	57.8 ± 6.7	44.9 ± 7.8
	27-OHC	0.037 ±	0.033 ±	0.071 ±	0.047 ±	0.77 ± 0.02	0.51 ± 0.15	0.076 ± 0.02	0.053 ± 0.01	0.051 ±	0.026 ±
	7-KC	0.74 ± 0.40	0.48 ± 0.26	0.59 ± 0.17	0.67 ± 0.15	0.032 ± 0.006	0.030 ± 0.008	0.53 ± 0.18	0.54 ± 0.15	0.52 ± 0.24	0.49 ± 0.19
	7β-OHC	0.36 ± 0.19	0.27 ± 0.14	0.42 ± 0.15	0.54 ± 0.22	0.24 ±	0.025 ± 0.007	0.21 ± 0.06	0.23 ± 0.06	0.24 ± 0.11	0.24 ± 0.11
	Cholesterol[a]	14.8 ± 1.3	13.3 ± 2.9	18.5 ± 3.4	19.9 ± 1.3	22.3 ± 3.5	23.3 ± 5.2	17.8 ± 2.1	18.5 ± 2.3	20.0 ± 2.4	20.1 ± 2.4
Cortex	Lathosterol	36.6 ± 9.7	27.0 ± 10.2	39.7 ± 9.3	18.3 ± 6.1	35.8 ± 9.5	17.5 ± 5.1	31.9 ± 9.5	15.2 ± 2.6	29.7 ± 5.6	15.0 ± 3.5
	Lanosterol	8.6 ± 2.6	7.8 ± 2.0	9.2 ± 3.2	6.4 ± 1.5	7.7 ± 2.4	4.5 ± 1.3	8.1 ± 2.6	4.4 ± 1.1	9.0 ± 1.2	5.0 ± 1.4
	Zymosterol	2.5 ± 0.55	2.8 ± 0.84	3.0 ± 0.6	2.7 ± 0.5	2.5 ± 0.4	1.9 ± 0.4	3.4 ± 1.1	2.7 ± 0.73	2.9 ± 0.39	2.0 ± 0.42
	24,25 diH lan.	0.39 ± 0.12	0.37 ± 0.12	0.34 ± 0.13	0.23 ± 0.09	0.32 ± 0.12	0.25 ± 0.15	0.24 ± 0.06	0.14 ± 0.04	0.32 ± 0.04	0.24 ± 0.07
	Desmosterol	31.3 ± 11.2	36.6 ± 9.2	34.1 ± 15.7	45.3 ± 17.0	35.3 ± 14.0	45.7 ± 5.5	30.9 ± 11.2	36.0 ± 10.7	32.4 ± 7.5	38.3 ± 3.2
	7-DHC	40.0 ± 12.6	40.1 ± 9.2	42.8 ± 6.4	45.3 ± 14.4	43.3 ± 6.5	45.3 ± 14.4	27.6 ± 7.7	30.9 ± 10.0	47.4 ± 6.4	50.0 ± 7.6
	24-OHC	27.5 ± 7.5	29.3 ± 7.5	30.1 ± 6.0	33.0 ± 5.1	39.6 ± 13.0	37.3 ± 6.5	31.0 ± 10.8	29.2 ± 6.9	46.1 ± 8.5	40.1 ± 5.6
	27-OHC	0.036 ±	0.032 ± 0.007	0.041 ±	0.043 ±	0.047 ±	0.044 ±	0.047 ± 0.02	0.035 ± 0.01	0.053 ± 0.007	0.039 ±
	7-KC	0.37 ± 0.18	0.33 ± 0.11	0.50 ± 0.12	0.48 ± 0.14	0.41 ± 0.17	0.54 ± 0.20	0.32 ± 0.08	0.29 ± 0.11	0.88 ± 0.53	0.90 ± 84
	7β-OHC	0.19 ± 0.11	0.20 ± 0.12	0.38 ± 0.14	0.36 ± 0.13	0.13 ±	0.16 ±	0.11 ± 0.02	0.16 ± 0.07	0.40 ± 0.30	0.22 ± 0.09
	Cholesterol[a]	10.1 ± 2.4	9.2 ± 2.5	15.4 ± 2.7	15.0 ± 2.1	11.0 ± 2.5	11.9 ± 1.7	11.4 ± 2.5	10.7 ± 1.7	15.5 ± 1.7	16.4 ± 3.1

24, 25 diH lan. = 24, 25 dihydro lanosterol; 7-DHC = 7-dehydrocholesterol; 24-OHC = 24(S)-hydroxycholesterol; 27-OHC = 27-hydroxycholesterol; 7-KC = 7-ketocholesterol; 7β-OHC = 7β-hydroxycholesterol. [a]Values expressed as µg/mg tissue.